

Adaptive Notch Filter Using Real-Time Parameter Estimation

Jason Levin, *Member, IEEE*, Néstor O. Pérez-Arancibia, *Member, IEEE*, and Petros A. Ioannou, *Fellow, IEEE*

Abstract—The control of flexible systems is often difficult due to the exact frequencies of the elastic modes being hard to identify. These flexible modes may change over time, or vary between units of the same system. The variation in the modal dynamics may cause a degradation in performance or even instabilities unless compensated for by the control scheme. Controllers designed for these types of systems use notch filters for suppression, however variation in the parameters of the flexible modes cause the need for wide notch filters. An adaptive scheme is proposed which uses an online estimator based on plant parameterization. Since the estimator is able to identify the modal dynamics, an adaptive notch filter is able to track an incorrectly modeled or varying flexible mode. The adaptive notch filter can be designed narrower, adding less phase lag at lower frequencies, thereby allowing an increase in bandwidth and disturbance rejection capability. Simulation and experimental verification of the adaptive mode suppression scheme is given through the use of a laser beam pointing system. The adaptive scheme is compared to a nonadaptive scheme, and is able to decrease the standard deviation of the experimentally measured tracking error by 14% even when the flexible dynamics are unknown.

Index Terms—Adaptive control, adaptive notch filter, laser-beam control.

I. INTRODUCTION

FLEXIBLE dynamics occur in numerous mechanical systems where control systems are desired to maintain stability or increase tracking performance. Unless accounted for by the control scheme, these dynamics can cause instabilities or degradation in performance. A notch filter is sometimes used to suppress the flexible modes, however in many applications the modal frequencies are often uncertain and can even vary over time creating the need for a wide notch filter. One such system is a pointing system, where the flexible actuators may cause the need for a notch filter. As the notch filter becomes wider it also induces greater magnitude and phase lag at lower frequencies resulting in a lower bandwidth system.

Manuscript received April 09, 2009; revised November 11, 2009; accepted March 18, 2010. Manuscript received in final form April 26, 2010. First published May 24, 2010; current version published April 15, 2011. Recommended by Associate Editor T. Zhang. This work was supported in part by NSF Award CMS-0510921 and NASA Grant NCC4-158.

J. Levin was with the Department of Electrical Engineering, University of Southern California, Los Angeles, CA 90089–2560 USA. He is now with General Atomics Aeronautical Systems, Inc., Poway, CA 92064 USA (e-mail: jason.levin@uav.com).

N. O. Pérez Arancibia is with the Mechanical and Aerospace Engineering Department, University of California, Los Angeles, CA 90095–1597 USA (e-mail: nestor@seas.ucla.edu).

P. A. Ioannou is with the Department of Electrical Engineering, University of Southern California, Los Angeles, CA 90089–2560 USA (e-mail: ioannou@usc.edu).

Color versions of one or more of the figures in this brief are available online at <http://ieeexplore.ieee.org>.

Digital Object Identifier 10.1109/TCST.2010.2049493

One solution to such a problem is the adaptive notch filter, a notch filter whose center frequency varies online to track the modal frequencies of the system. The adaptive notch filter has been studied in signal processing research [1]–[3] as well as various applications, such as the hard disk drive (HDD) [4], launch vehicles [5], aircraft [6], and space structures [7]. The adaptive notch filter presented in [5] is used on the model of a booster from the Advanced Launch System (ALS) program. The least squares estimator in the publication uses a simple undamped resonator as the model for estimation and functions well since the resonant mode is very pronounced. However in other applications, full plant parameterizations is necessary as the flexible mode may not be as significant. Another strategy for the estimation of the center frequency can be found in [4], where frequency weighting functions are used. The downside is there are several failure modes that are known and avoidance requires some modal information *a priori*. A stochastic state space algorithm for mode frequency estimation is presented in [6]; however it relies on the injection of a probe signal which is not needed in the scheme presented here. The indirect adaptive compensation (IAC) scheme in [8] also requires a probe signal to complete the estimation. The adaptive mode suppression scheme in [7] uses a LMS algorithm to update filter coefficients and then the modal parameters are extracted from the filter. This is opposite as to what is being presented in this brief, where the modal parameters are first estimated and then used in the adaptive notch filter.

This brief presents a feedback control scheme which makes use of an adaptive notch filter. The adaptive notch filter is designed to suppress the modal dynamics of the system while working in harmony with another controller designed for the rigid system, that is the system without the flexible modes. This second controller, called the rigid-body controller, can be designed using a variety of methods since the elastic dynamics can be, for the most part, neglected in the design. In this brief, we will present a design requirement, on the interaction of the rigid-body control and adaptive notch filter, which ensures stability of the closed-loop adaptive system. Since the design of each component can be done in a more separated method it may be useful for systems where the modes are not precisely known early in the control design process or for systems where the modal parameters vary between production units. This brief makes a relevant contribution when compared to past research and publications on adaptive notch filtering for numerous reasons. In the past signal processing research the adaptive notch filters are not used in closed-loop feedback control schemes, so the stability and performance for control is not reported or analyzed. However, in this brief we present the requirements for closed-loop stability and demonstrate performance on an experimental application. Unlike past publications, we explicitly give the design requirements for the rigid-body controller and the interaction of the adaptive notch filter with such a controller. Also

the scheme presented herein does not need persistent excitation [9] or a probe signal, which other published schemes require.

The design procedure for the adaptive notch filter scheme is given to serve as an example for other future designs. To showcase the ability of the adaptive notch filter to work in a real-time control system the laser-beam pointing experiment of [10] will be used. In this experiment, the plant contains a single lightly damped complex pole. This type of system is prevalent in mechanical systems which, by design, have a flat response below the bandwidth of the elastic modes. The adaptive notch filter enables a higher bandwidth control system with better performance, in terms of disturbance rejection capabilities. Other methods of rigid-body control with an adaptive notch filter of this type are a LQR controller for aircraft control in [11] and a classical phase lead design for an HDD in [12]. It should be noted that the complete stability analysis will be presented in an upcoming publication and the notation used in this brief will be very similar to that of [9]. The general adaptive notch filter control scheme is given in Section II. The control design for the single complex pole is presented in Section III and then simulations and experiments of the design are discussed in Section IV. Finally conclusions are drawn in Section V.

II. GENERAL ADAPTIVE NOTCH FILTER

The setup for this problem is a rigid plant with a single unknown lightly damped flexible mode which only contains a single pair of complex poles. A controller is designed to achieve good performance in the presence of disturbances, which means shaping the sensitivity and complementary sensitivity functions appropriately. The control objective may include tracking a certain class of reference signal $y_m \in \mathcal{L}_\infty$ by using the internal model principle. So, we design the controller to include $Q_m(s)$, which is an internal model of y_m and is a known monic polynomial of degree q with all roots in $\Re[s] \leq 0$ and with no repeated roots on the $j\omega$ -axis. The plant takes the form

$$y_p = G_p(s)M(s)u_p + d = \frac{Z_p(s)}{R_p(s)} \frac{Z_m(s)}{R_m(s)} u_p + d \quad (1)$$

where $Z_m(s)/R_m(s)$ is a mode of the plant, $Z_p(s)/R_p(s)$ is the non-modal part of the plant, and d is a bounded output disturbance. The flexible part of the plant takes the form

$$\frac{Z_m(s)}{R_m(s)} = \frac{\omega_d^2}{s^2 + 2\zeta\omega_d s + \omega_d^2} \quad (2)$$

where $\zeta > 0$ is the damping and $\omega_d > 0$ is the natural frequency of the mode. It is assumed that the order of $R_p(s)$ is n , and since we are concerned with suppressing the flexible modes, the non-modal part of the plant $G_p(s) = Z_p(s)/R_p(s)$ must be stabilizable so a rigid-body controller, later denoted as $C(s)$, can be designed for the rigid system.

A. Known Parameter Case

The control scheme includes a narrow adaptive notch filter centered at the natural frequency of the flexible pole in (1), and a compensator designed for $G_p(s)$ using any design technique

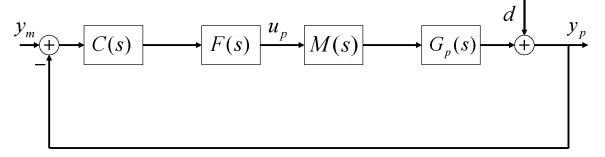


Fig. 1. Feedback system diagram for the mode suppression schemes.

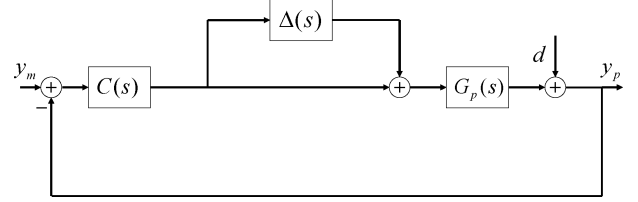


Fig. 2. Feedback system diagram with the notch filter and mode expressed as an uncertainty $\Delta(s)$.

while, for the most part, completely neglecting the flexible dynamics. Here we design a controller which includes an internal model $Q_m(s)$, however this is not necessary for the adaptive notch filter to function properly. We pose the control problem in this format for clarity of presentation, the rigid-body control design is not the main topic of importance in this brief. The control loop is seen in Fig. 1 and input

$$u_p = -F(s)C(s)(y_p - y_m) \quad (3)$$

$$C(s) = \frac{P(s)}{Q_m(s)L(s)} \quad (4)$$

$$F(s) = \frac{Z_f(s)}{R_f(s)}. \quad (5)$$

We assume that the rigid-body controller $C(s)$ is proper and realizable, and is designed such that the polynomial equation

$$L(s)Q_m(s)R_p(s) + P(s)Z_p(s) = A(s) \quad (6)$$

gives a Hurwitz $A(s)$, which are the desired closed-loop poles when the flexible dynamics and notch filter are neglected. The filter $F(s)$ in (3) is

$$\frac{Z_f(s)}{R_f(s)} = \frac{s^2 + 2\zeta_z\omega_d s + \omega_d^2}{s^2 + 2\zeta_r\omega_d s + \omega_d^2} \quad (7)$$

where ω_d is the same as in (2), $\zeta_z, \zeta_r > 0$, and $\zeta_z < \zeta_r$. We would like to design the filter to fully suppress the flexible mode at the resonant frequency, this gives us a condition that must be met

$$\left| \frac{Z_m(j\omega)Z_f(j\omega)}{R_m(j\omega)R_f(j\omega)} \right| \leq k_m \quad (8)$$

where k_m is the desired margin. Now treating the modes and notch filter as uncertainty, and ignoring the disturbance, the system can be put into the form of Fig. 2, whose characteristic equation is

$$1 + C(s)G_p(s)(1 + \Delta(s)) = 0 \quad (9)$$

which, due to the stable roots of $1 + C(s)G_p(s) = 0$, implies

$$1 + \frac{C(s)G_p(s)}{1 + C(s)G_p(s)}\Delta(s) = 0. \quad (10)$$

Taking the above equation and substituting in the polynomials and applying the small gain theorem the following must be satisfied:

$$\left\| \frac{P(s)Z_p(s)}{A(s)}\Delta(s) \right\|_{\infty} < 1 \quad (11)$$

$$\Delta(s) = F(s)M(s) - 1. \quad (12)$$

We use this form of the uncertainty in (12) for ease of the stability proof which will be presented in a future publication. It can be shown that the tracking error $e_1 = y_p - y_m$ is

$$e_1 = -\frac{L(s)R_p(s)}{Q_m(s)L(s)R_p(s) + P(s)Z_p(s)(1 + \Delta(s))}Q_m y_m + \frac{L(s)R_p(s)}{Q_m(s)L(s)R_p(s) + P(s)Z_p(s)(1 + \Delta(s))}Q_m d \quad (13)$$

which is a proper stable transfer function since (11) is satisfied. Now we have

$$e_1 = -\frac{L(s)R_p(s)}{Q_m(s)L(s)R_p(s) + P(s)Z_p(s)(1 + \Delta(s))}Q_m d + \varepsilon_t \quad (14)$$

where ε_t is a term exponentially decaying to zero. Therefore the control law will cause e_1 to converge exponentially to the set

$$D_e = \{e_1 \mid \|e_1\| \leq cd_0\} \quad (15)$$

where d_0 is an upper bound for $|d|$ and $c > 0$ is a constant. It should be noted this result is for the system when all the parameters are known and the requirement in (11) is met.

B. Estimation of Plant Parameters

The adaptive mode suppression scheme that is used when the flexible dynamics are uncertain or changing will now be designed. Starting with the system in (1) we have

$$y_p = \frac{Z_p(s)}{R_p(s)} \frac{Z_m^*(s)}{R_m^*(s)} u_p + d \quad (16)$$

where $Z_m^*(s)/R_m^*(s)$ is the unknown mode of the plant

$$\frac{Z_m^*(s)}{R_m^*(s)} = \frac{\omega_d^{*2}}{s^2 + 2\zeta^* \omega_d^* s + \omega_d^{*2}} \quad (17)$$

and $Z_p(s)/R_p(s)$ is the known part of the plant. $Z_p(s)$, $R_p(s)$, $Z_m^*(s)$, and $R_m^*(s)$ follow all the same assumptions made in the known parameter case. The polynomials denoted with the star are polynomials whose coefficients are the actual values of the real system, which are treated as unknown. Similarly, the parameters with a star are the actual parameters of the system. The parametric model to estimate the unknown modal frequency is as follows:

$$z = \theta^{*T} \phi + \eta \quad (18)$$

where η is the used to represent the disturbance where

$$\eta = \frac{R_p(s)R_m^*(s)}{\Lambda_p(s)} d \in \mathcal{L}_{\infty} \quad (19)$$

$$z = \frac{s^2 R_p(s)}{\Lambda_p(s)} y_p \quad (20)$$

$$\phi = \left[\frac{-sR_p(s)}{\Lambda_p(s)} y_p \quad \frac{Z_p(s)}{\Lambda_p(s)} u_p - \frac{R_p(s)}{\Lambda_p(s)} y_p \right]^T \quad (21)$$

$$\theta^* = [2\zeta^* \omega_d^* \quad \omega_d^{*2}]^T \quad (22)$$

and $\Lambda_p(s)$ is a monic Hurwitz polynomial of degree $n + 2$. The parametric model in (18) is achieved by taking (16) and (17), multiplying by a common denominator, collecting unknown terms, and then making proper transfer functions by dividing by a Hurwitz polynomial $\Lambda_p(s)$. The creation of this type of parametric model is well documented in [9] and the exact representation of the flexible modes in this form allows for estimation of the unknown modal parameters.

Our goal is to estimate the modal frequency and damping. A wide class of adaptive laws can be used to estimate the unknown parameters, but we adopt the gradient algorithm with parameter projection and a deadzone. Allow $\phi = [\phi_1, \phi_2]^T$, $\theta = [\theta_1, \theta_2]^T$, and also some *a priori* known bounds on the damping and natural frequency such that $1 \geq \zeta^u \geq \zeta^* \geq \zeta^l > 0$ and $\omega_d^u \geq \omega_d^* \geq \omega_d^l > 0$ are satisfied. These bounds are used for projection and can be determined with some knowledge of the actual system and where the parameters may lie. The size of the bounds only effects the robustness of the design. A deadzone modification is added to ensure robust adaptation in the presence of the bounded disturbance. The update equations are

$$\dot{\theta}_1 = \begin{cases} \gamma_1(\varepsilon + g)\phi_1, & \text{if } (2\zeta^u \omega_d^u > \theta_1 > 2\zeta^l \omega_d^l) \\ & \text{or } (\theta_1 = 2\zeta^l \omega_d^l \text{ and } \varepsilon \phi_1 \geq 0) \\ & \text{or } (\theta_1 = 2\zeta^u \omega_d^u \text{ and } \varepsilon \phi_1 \leq 0) \\ 0, & \text{otherwise} \end{cases} \quad (23)$$

$$\dot{\theta}_2 = \begin{cases} \gamma_2(\varepsilon + g)\phi_2, & \text{if } ((\omega_d^u)^2 > \theta_2 > (\omega_d^l)^2) \\ & \text{or } (\theta_2 = (\omega_d^l)^2 \text{ and } \varepsilon \phi_2 \geq 0) \\ & \text{or } (\theta_2 = (\omega_d^u)^2 \text{ and } \varepsilon \phi_2 \leq 0) \\ 0, & \text{otherwise} \end{cases} \quad (24)$$

$$\varepsilon = \frac{z - \theta^T \phi}{m_s^2} \quad (25)$$

$$m_s^2 = 1 + \phi^T \phi. \quad (26)$$

$$g = \begin{cases} 0, & \text{if } |\varepsilon m_s| > g_0 \\ -\varepsilon, & \text{if } |\varepsilon m_s| \leq g_0. \end{cases} \quad (27)$$

In the above equations the overdot represents the differential operator and the bounds $\zeta^l, \zeta^u, \omega_d^l, \omega_d^u$ are constants determined *a priori*, and $\gamma_1, \gamma_2, g_0 > 0$ are also design parameters chosen *a priori*. The deadzone will ensure that adaptation stops when the estimation error is below the level of the disturbance, so that only good information is used to update the parameters. The above estimation law guarantees the following:

- 1) $\theta \in \mathcal{L}_{\infty}$;
- 2) $\varepsilon, \varepsilon m_s, \dot{\theta} \in S(g_0 + \eta^2/m_s^2)$;
- 3) $\dot{\theta} \in \mathcal{L}_1 \cap \mathcal{L}_2$;
- 4) $\lim_{t \rightarrow \infty} \theta(t) = \bar{\theta}$, where $\bar{\theta}$ is a constant vector.

C. Adaptive Control Law

The adaptive control law is formed by replacing the notch filter in (3), which has the form of (7), with an adaptive notch filter. The online estimates used in the adaptive notch filter come from the online estimator and are

$$\theta = [2\hat{\zeta}_d\hat{\omega}_d \quad \hat{\omega}_d^2]^T. \quad (28)$$

The adaptive control law becomes

$$u_p = -\frac{\hat{Z}_f(s) P(s)}{\hat{R}_f(s) L(s) Q_m(s)} (y_p - y_m). \quad (29)$$

In the above control law, the notch filter $\hat{Z}_f(s)/\hat{R}_f(s)$ is designed to cancel the unknown mode of the plant $Z_m^*(s)/R_m^*(s)$. By denoting the polynomials with a *hat* we are saying the coefficients are time-varying estimates which come from the online estimator. This is done by using the estimate of the modal frequency as the center frequency thereby making it an adaptive notch filter. The filter becomes

$$\frac{\hat{Z}_f(s)}{\hat{R}_f(s)} = \frac{s^2 + 2\zeta_z\hat{\omega}_d s + \hat{\omega}_d^2}{s^2 + 2\zeta_r\hat{\omega}_d s + \hat{\omega}_d^2} \quad (30)$$

where $\hat{\omega}_d$ is the estimate of the modal frequency and the damping ratios are set a priori using (8) as a reference.

We also must make sure that (11) is satisfied at every frozen time t , which leads to

$$\left\| \frac{P(s)Z_p(s)}{A^*(s)} \cdot \Delta(s, \theta) \right\|_{\infty} < 1 \quad (31)$$

$$\Delta(s, \theta) = \hat{F}(s, \theta) \cdot \hat{M}(s, \theta) - 1. \quad (32)$$

By frozen time we mean that the time-varying coefficients of the polynomials are treated as constants when two polynomials are multiplied. Therefore the controller $C(s)$ must be designed such that (31) is always satisfied. This implies *a priori* knowledge of the bounds on the unknown parameters which leads to a convex set $\theta \in S$, that the estimator must use for projection. These bounds, through the updating of the parameters in the adaptive notch filter, create a convex set of possible $\Delta(s, \theta)$ which we use to obtain a weight $W(s)$ used for control design. Now, denote $\bar{F}(s, \theta)$, $\bar{M}(s, \theta)$ as the frozen time versions of the systems $\hat{F}(s, \theta)$, $\hat{M}(s, \theta)$. That is to say, the overbar versions have estimated parameters that come from the set S but are frozen in time, and therefore are treated as LTI systems. We have

$$l(\omega) = \max_{\theta \in S} |\bar{F}(j\omega, \theta)\bar{M}(j\omega, \theta) - 1| \quad (33)$$

and a rational transfer function weight

$$|W(j\omega)| \geq l(\omega), \quad \forall \omega. \quad (34)$$

This weight can be substituted in (31) to acquire the LTI stability requirement as

$$\left\| \frac{C(s)G_p(s)}{1 + C(s)G_p(s)} W(s) \right\| = \left\| \frac{P(s)Z_p(s)}{A^*(s)} W(s) \right\|_{\infty} < 1. \quad (35)$$

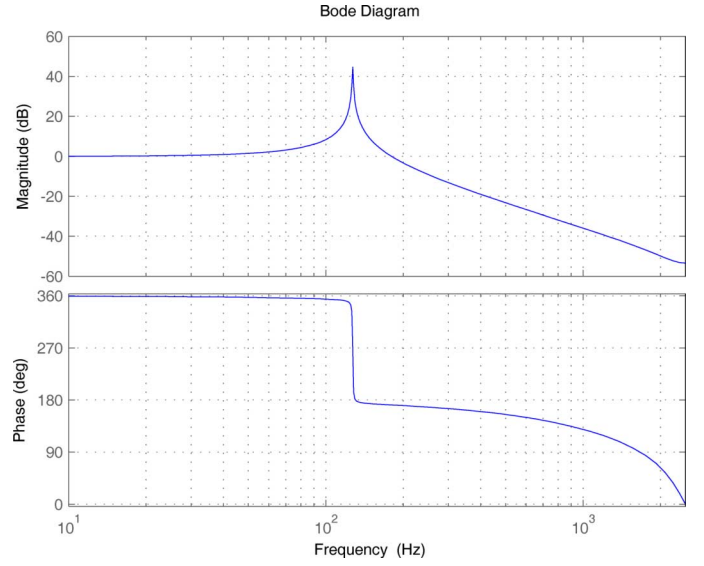


Fig. 3. Bode plot of the open loop plant. A single decoupled axis of the FSM experimental setup.

This requirement for stability can be achieved offline from knowledge of the parameter bounds and the adaptive notch filter design. This stability requirement is used in a future publication where an analytical proof is described in which proves boundedness of the parameters as well as convergence of the error signal to zero. However there is no guarantee that the estimated parameters will converge to the true values, as this is not needed for stability. However if the reference signal contains significant persistent excitation (PE) [9], then the estimates will converge to the true values. In other words, the parameters will adapt to bring the error signal close to zero, at which point the deadzone modification will halt adaptation, thereby freezing the estimates which may not be at the true value.

III. CONTROL DESIGN

The adaptive notch filter scheme will now be designed for a system with a single complex pole, which is representative of mechanical systems with a flat frequency response up to the frequency of a lightly damped elastic mode. This type of system is similar to that of the MEMS fast steering mirror (FSM) which will be used as the actuator in the simulations and experiments described later. For this system the rigid part of the plant $G_p(s)$ is unity and the modal part is as in (17) leading to a system with a bode plot seen in Fig. 3. For this section we will allow the control design to be done in the Laplace domain and in the next section the controllers will be discretized for implementation on a digital computer.

Some fictitious stability and performance requirements are created to show the benefit of the adaptive mode suppression scheme. Since our goal is perfect tracking and elimination of disturbances, the chosen performance metric will be the standard deviation of the tracking error. Therefore requirements are levied on the closed loop sensitivity function which are a magnitude of at most -55 dB at 1 Hz and a maximum magnitude

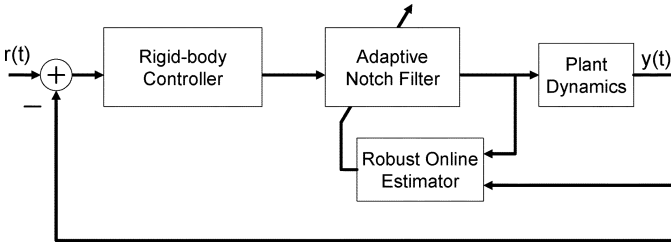


Fig. 4. Closed-loop diagram for the experimental setup. For the non-adaptive scheme the adaptive notch filter is replaced by a fixed notch filter and the online estimator is removed. Here $r(t)$ is the reference signal which is equal to zero and $y(t)$ is the measured output.

of 12 dB. Now a requirement will be added to limit the bandwidth of the closed loop system, this may be necessary for a variety of reasons. In a real implemented system used for commercial use, the sampling rate of the feedback error signal may be only slightly faster than the flexible dynamics and high frequency noise may be present, so a limited bandwidth would be desired. These factors contribute to the requirement of limiting the closed loop complementary sensitivity to at most -60 dB at 500 Hz with an overall maximum value of 12 dB.

With these requirements in place, two controllers will be designed and the closed loop diagram is in Fig. 4. A control scheme utilizing an adaptive notch filter (ANF) and a scheme with a fixed non-adaptive notch filter (NA) will be created. The non-adaptive scheme will utilize a wide notch filter to account for variations in the flexible mode frequency of up to 5% and variations of the damping of up to 5%. This wider notch filter will add phase lag at the lower frequencies and limit the performance of the system. However the adaptive scheme will have a much narrower notch filter, adding less phase lag and thereby allowing for better disturbance rejection. Both of the notch filters are displayed in Fig. 5. The frozen time adaptive notch filter is

$$\bar{F}_A(s, \theta) = \frac{s^2 + 2(9.6 \times 10^{-4})\sqrt{\theta_2}s + \theta_2}{s^2 + 2(0.38)\sqrt{\theta_2}s + \theta_2} \quad (36)$$

and the non-adaptive notch filter is

$$F_{NA}(s) = \frac{s^2 + 2(1.0 \times 10^{-3})(799.64)s + (799.64)^2}{s^2 + 2(1.0)(799.64)s + (799.64)^2}. \quad (37)$$

To graphically visualize the benefit of the narrower adaptive notch filter we will go back to the stability requirement where the notch filter and flexible mode are treated as uncertainties. If we allow the unknown parameters to come from the set S , which is created from the a priori bounds on the unknown parameters, we can devise a covering function for both the adaptive and non-adaptive cases. First for the adaptive case we will create the filter $W_A(j\omega)$ by using (33) and (34) and the bounds specified by the 5% variation in natural frequency and damping. For this we use the adaptive notch filter given in (36), which is treated as a frozen time LTI system when θ is constant, and the mode given by

$$\bar{M}(s, \theta) = \frac{\theta_2}{s^2 + \theta_1 s + \theta_2}. \quad (38)$$

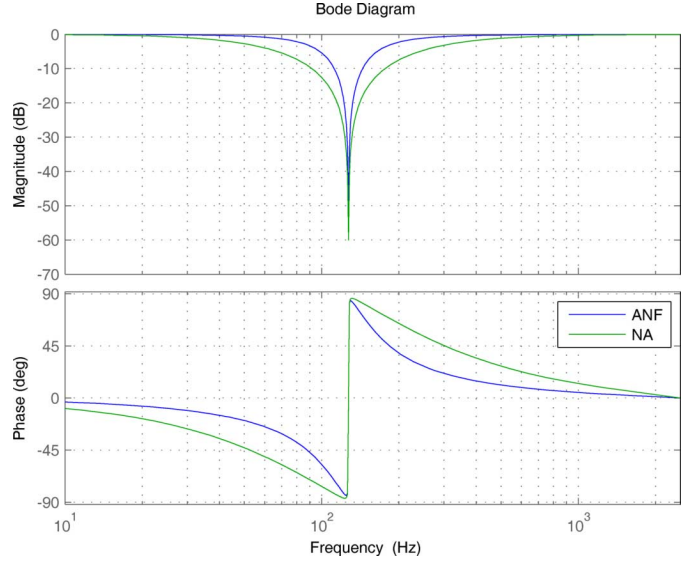


Fig. 5. Bode plot of the notch filters. The narrower ANF adds less phase lag than the non-adaptive notch filter (NA). The ANF is one where the center frequency is frozen at the same value as the non-adaptive notch filter, therefore it can be treated as LTI.

For the non-adaptive notch filter case we will construct the filter $W_{NA}(j\omega)$ by using

$$l_{NA}(\omega) = \max_{\theta \in S} |F_{NA}(j\omega, \theta)\bar{M}(j\omega, \theta) - 1| \quad (39)$$

and then

$$|W_{NA}(j\omega)| \geq l_{NA}(\omega), \quad \forall \omega \quad (40)$$

where the NA subscript is used to denote the non-adaptive scheme. The stability criteria in (35) can now be used in the form of

$$|T(j\omega)| < \left| \frac{1}{W(j\omega)} \right|, \quad \forall \omega \quad (41)$$

where $T(s)$ is the complementary sensitivity function. Plotting the bode plots of the inverse of the filters $W_A(s)$ and $W_{NA}(s)$ in Fig. 6 shows how the adaptive system can allow an increase in bandwidth as well as disturbance rejection. It should also be noted that the adaptive notch filter can deal with a much larger variation in damping since the center frequency will track the flexible mode and suppress the mode. However the suppression capabilities of the fixed non-adaptive notch filter decrease exponentially as the actual modal frequency of the plant is displaced from the center frequency of the notch filter.

The rigid body controller for the two cases are slightly different, the adaptive scheme has a slightly higher gain and faster zeros allowing for an increase in performance while still meeting the requirements, which is permitted due to the narrower adaptive notch filter. Both rigid body controllers are designed to maximize performance for the given notch

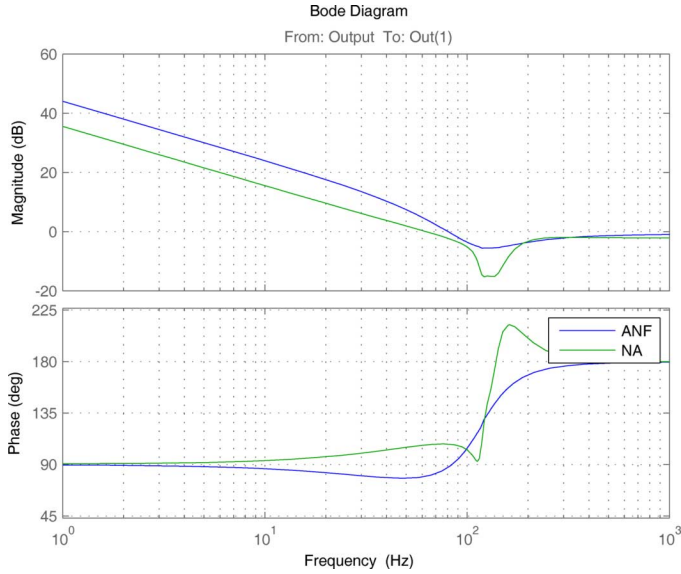


Fig. 6. Bode plot of inverse of the filters $W_A(s)$ and $W_{NA}(s)$. The narrower ANF has a looser constraint on the rigid body control design, when compared to the non-adaptive notch filter (NA).

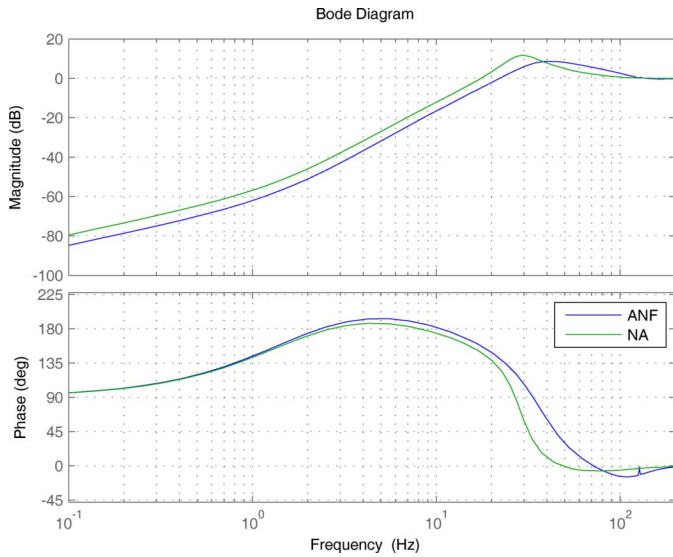


Fig. 7. Bode plot of the closed-loop sensitivity functions. The narrower ANF allows for better disturbance rejection than the non-adaptive notch filter (NA) due to the increase in bandwidth of the rigid body controller. The ANF can be treated as LTI since we fix the value for the center frequency to be the same value used in the non-adaptive notch filter, which is the nominal plant modal frequency.

filters in their respective schemes using classical SISO design methodologies. The rigid controllers are

$$C_{ANF}(s) = \frac{129609.0(s + 75.66)^2}{s(s + 635.8)(s + 10.87)(s + 9.86)} \quad (42)$$

$$C_{NA}(s) = \frac{107090.6(s + 61.44)^2}{s(s + 635.8)(s + 10.87)(s + 9.86)} \quad (43)$$

where $C_{ANF}(s)$ is the rigid controller for the adaptive notch filter scheme and $C_{NA}(s)$ is the rigid controller for the non-adaptive scheme. The sensitivity functions of each scheme is seen in Fig. 7 where the disturbance rejection capability of the

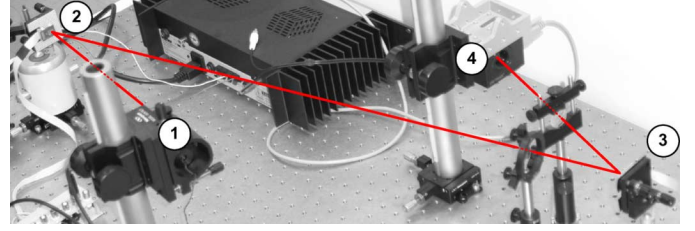


Fig. 8. Photograph of the laser beam system.

adaptive scheme is clear. Since the adaptive notch filter is narrower than the non-adaptive counterpart, the rigid controller can be designed more aggressively causing the lower magnitude of the sensitivity function. The closed loop bandwidth of the adaptive scheme is also slightly higher at 65 Hz as opposed to that of the non-adaptive scheme which has a bandwidth of 51 Hz, although both schemes meet the sensitivity and complementary sensitivity function requirements that were imposed. With the controllers and notch filters designed, using the bounds for the unknown parameters, we can check the stability condition of (35) using the $W_A(j\omega)$ and $W_{NA}(j\omega)$ covering filters created earlier. Both schemes have greater than 7 dB of gain margin, however to meet the performance requirements and tolerance on the flexible mode, the phase margins suffer. The non-adaptive scheme has a phase margin of 18 degree while in the ideal situation, with the parameters frozen, the adaptive scheme has a phase margin of 25 degrees. The LTI margins for the adaptive scheme is not a realistic quantity, however it is discussed here to show how the margins are better when a notch filter is narrower.

The online estimator is designed for the adaptive scheme in the same way presented in the previous section. The $\Lambda_p(s)$ filter is designed to maximize the signal to noise content of the estimator, this can be done by designing bandpass filters in regions where the flexible modal frequency is thought to occur. The deadzone modification is the estimator will turn off estimation when the estimation error becomes less than some designated preset design value. This is necessary due to the disturbance signal, which will cause the estimates to drift based on incorrect estimation information.

IV. SIMULATIONS AND EXPERIMENTS

The simulations presented in this section use the dynamical models of the laser-beam system shown in Fig. 8, where the plant displays a lightly damped flexible mode. The details of the experimental setup in Fig. 8 are described in [10], however, a brief overview is given here.

As shown in the photograph in Fig. 8, a laser beam leaves the source at position ①, reflects off the fast steering mirror FSM-C at position ②, then reflects off the fast steering mirror FSM-D at position ③ and finally reaches the optical position sensor at position ④. Two lenses in the optical path focus the beam on FSM-D and the sensor. The mirrors FSM-C and FSM-D are identical Texas Instruments (TI) MEMS mirrors used in laser communications for commercial and defense applications. FSM-C is the control actuator, and FSM-D is used to add disturbance.

The open-loop discrete-time plant of the system is the transfer function that maps the two-channel digital control command to

the sampled two-channel output of the optical position sensor. Thus open-loop plant of the system is the two-input/two-output digital transfer function for the lightly damped fast steering mirror FSM-C with a gain determined by the optical position sensor and the laser path length. Output channels 1 and 2 represent horizontal and vertical displacements, respectively, of the beam; input channels 1 and 2 represent commands that drive FSM-C about its vertical and horizontal axes, respectively.

As shown in [10], the two channels of the system can be decoupled, creating two separate SISO systems. Only Channel 1 will be used in the simulations considered here, because the results of this brief pertain to a single SISO system. A model of Channel 1, identified with a sample-and-hold rate of 5 kHz, is shown in Fig. 3, where the lightly damped flexible mode at 127 Hz can easily be observed. Notice, that the magnitude of the frequency response of Channel 1 at 0 Hz is 0 dB. This is due to the fact that the transfer function of Channel 1 has been scaled, so that, changes in the distances between the components in optical path in Fig. 8 do not change the models of the system.

A slightly different configuration to the one in Fig. 8, but with the same mirrors FSM-C and FSC-D (i.e., essentially the same dynamics), is used for the experiments to be described in Section IV-B. There, the effectiveness of the proposed adaptive mode suppression scheme is demonstrated. In this case, the closed-loop system is run with a sampling-and-hold rate of 5 kHz. Although the sampling frequency of the system is 5 kHz, a commercial application of the FSM may have a sampling frequency that is significantly smaller, due to time associated with the response of the detector, processing of the detector signal, or calculation of the position error.

Since the controllers, notch filters, and estimator are all designed in the continuous-time domain, they must be discretized for implementation on the real-time system at the sampling frequency of 5 kHz, since this was the given sampling rate of the system. Other sample rates were not tested, however a sampling rate much faster than the flexible dynamics of the system is needed for good performance. This is done using the bilinear transformation on both rigid controllers as well as the estimator filters, however the non-adaptive notch filter is discretized using the matched pole-zero technique [13]. The adaptive notch filter is converted to a digital notch filter for use in the real-time system by the following method. Allow

$$\omega_f = \tan\left(\frac{\hat{\omega}_d t_s}{2}\right) \quad (44)$$

where t_s is the sampling time. Then calculate the following values:

$$a_0 = 1 + 2\zeta_r \omega_f + \omega_f^2 \quad (45)$$

$$a_1 = 2\omega_f^2 - 2 \quad (46)$$

$$a_2 = 1 - 2\zeta_r \omega_f + \omega_f^2 \quad (47)$$

$$b_0 = 1 + 2\zeta_z \omega_f + \omega_f^2 \quad (48)$$

$$b_1 = 2\omega_f^2 - 2 \quad (49)$$

$$b_2 = 1 - 2\zeta_z \omega_f + \omega_f^2 \quad (50)$$

and the digital notch filter becomes

$$\hat{F}(z) = \left(\frac{a_0 + a_1 + a_2}{b_0 + b_1 + b_2}\right) \frac{b_0 z^2 + b_1 z + b_2}{a_0 z^2 + a_1 z + a_2}. \quad (51)$$

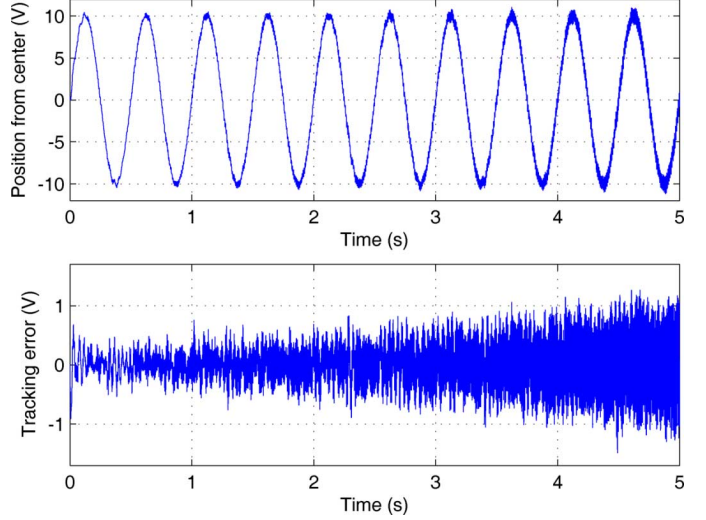


Fig. 9. Simulation results for the non-adaptive scheme when the notch filter is placed at 93% of the plant's modal frequency. *Top plot*: Position output y_p . *Bottom plot*: Tracking error. (ANF).

This filter can be implemented in a real-time system in a number of ways. Here the filter is placed in a canonical state space form and the states are updated using the standard discrete state space equations. Both rigid controllers are discretized using the same method, however the notch filters differ only slightly. The method given here for the adaptive notch filter is very similar to a matched pole-zero technique. Since the sampling frequency is much faster than the center frequencies of the notch, the discretization method does not play a vital role, but instead is only used for ease of online computation.

A. Simulations

A series of simulations are first completed using Matlab and Simulink, where the goal is to test the adaptive notch filter scheme before running real-time experiments. The disturbance that will be generated with the second FSM-D in the experiment is incorporated into the simulation. For the simulations the reference signal is a slowly varying 2 Hz sinusoid with an amplitude of 10 V. The adaptive mode suppression scheme is compared to the non-adaptive control scheme that is described previously, for both simulations the flexible modal frequency is thought to be at 93% of the nominal value, therefore the notch filters are centered at this incorrect frequency. At this amount of variation in modal frequency, the non-adaptive scheme will be unstable, as the notch filter is only meant to suppress a variation of up to 5%. The time series plots of the output and tracking error are displayed in Fig. 9, where the system begins to grow unstable as the flexible mode is not adequately suppressed. However, the adaptive scheme's output and tracking error are seen in Fig. 10. Here the system displays a large tracking error initially as the notch center frequency is incorrect, but as adaptation occurs the notch filter is able to suppress the mode thereby retaining performance and stability. The estimated modal frequency and estimation error are seen in Fig. 11.

B. Experiments

The experiments are conducted on the same day and run several times for further verification of the results. In Fig. 12 the time series of the error signal when the adaptive scheme is run

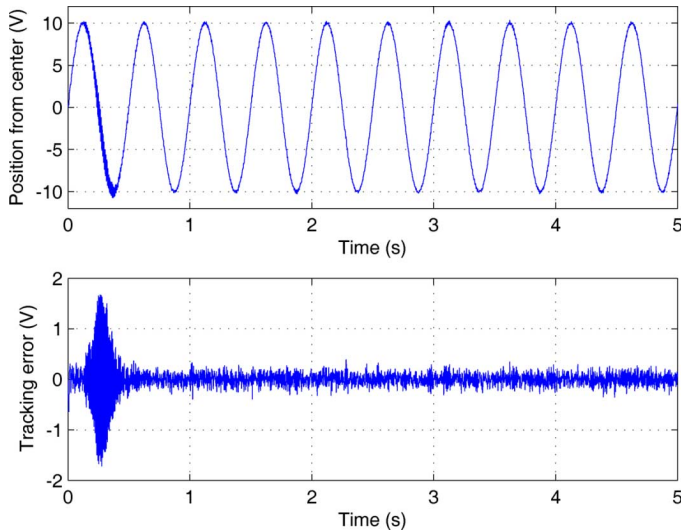


Fig. 10. Simulation results for the adaptive scheme when the initial value of the estimated modal frequency $\hat{\omega}_d$ is placed at 93% of the plant's modal frequency. *Top plot:* Position output y_p . *Bottom plot:* Tracking error. (ANF).

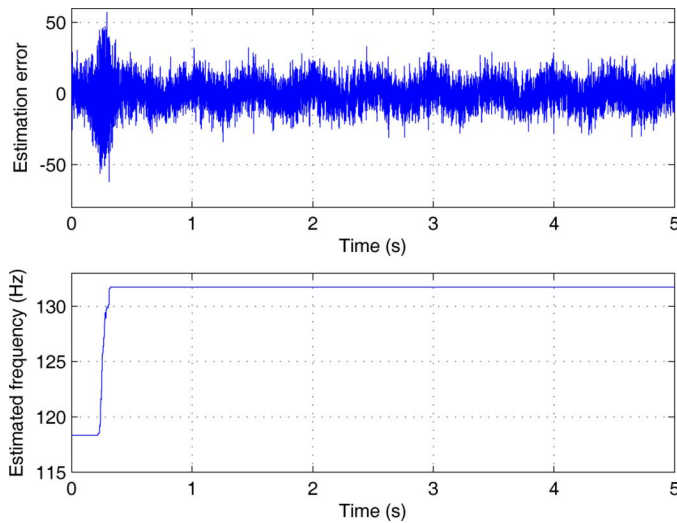


Fig. 11. Simulation results for the adaptive scheme. the actual modal frequency is 127.26 Hz. *Top plot:* Estimation error. *Bottom plot:* Estimated modal frequency.

is displayed. For the first 5 s the system is open loop, so only the disturbance created by FSM-D is seen in the error signal. The initial estimate of the plant's modal frequency is assumed to be at 95% of the actual value, thereby placing the adaptive notch filter in the incorrect location. This variation could be due to environmental effects, variations between FSMs, or degradation over time. Since the notch filter center frequency is incorrect, the flexible mode is excited and creates a large error shortly after the loop is closed. Adaptation then occurs, the notch filter tracks the modal frequency, the flexible mode is suppressed, and the error signal attenuates. As compared to a non-adaptive scheme, when the non-adaptive notch filter is placed perfectly (i.e., the plant model is correct and exactly known), the adaptive scheme decreases the standard deviation of the error signal by 14%. This increase in performance is due to the more aggressive rigid-body controller associated with the narrow adaptive notch filter.

The power spectral densities (PSDs) of error signal from the open loop system, adaptive scheme after adaptation, and non-

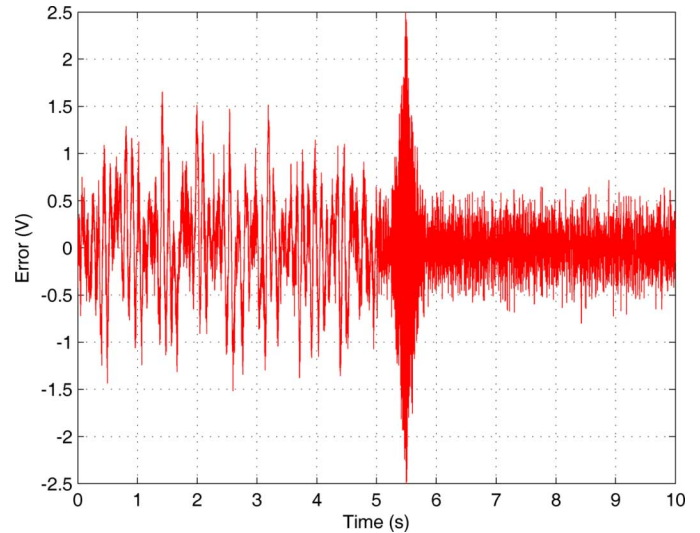


Fig. 12. Time series from the FSM experiment, the adaptive notch filter is initially placed at 95% of the actual modal frequency of the plant, however the adaptive notch filter will update the center frequency online. The control loop is closed at 5 s.

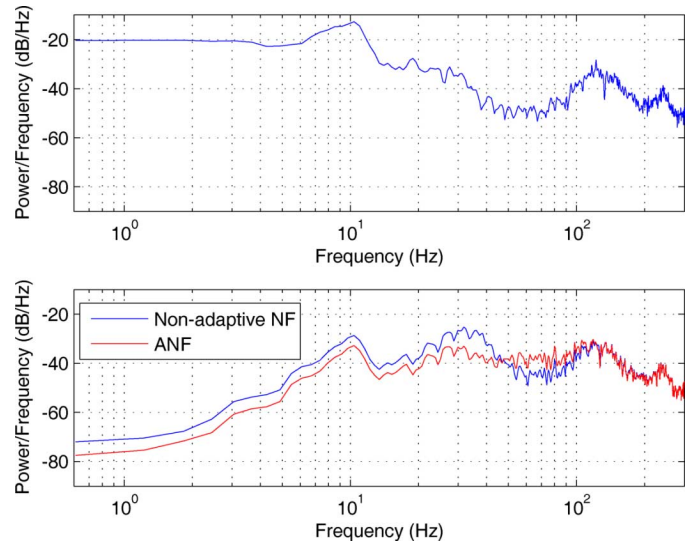


Fig. 13. PSDs computed from the error signal of the FSM experiment. The data used is collected from the 10 s mark until the 25 s mark. *Top plot:* Open-loop system, only disturbance. *Bottom plot:* Non-adaptive scheme and ANF.

adaptive scheme are presented in Fig. 13. The bottom plot displays the rejection of the disturbance with the adaptive scheme. Fig. 14 shows the estimation error and estimated modal frequency for the adaptive scheme. The plots are time series which begin at 5 s into the experiment, which is the time at which the loop is closed and the adaptive control scheme is turned on. Initially the estimated modal frequency, and therefore notch center frequency, is incorrect. This causes the system to be unstable and the tracking error to grow large, which in turn causes the estimation error to grow larger than the disturbance level. This level of excitation is sufficient enough to cause the online estimator to begin adapting the parameters online. Once the level of the error decreases below the deadzone threshold the estimation is halted and the parameters remain constant. It should also be noted that the estimated frequency does not exactly converge to the real plant modal frequency, but this is acceptable since the system becomes stable and the performance is improved.

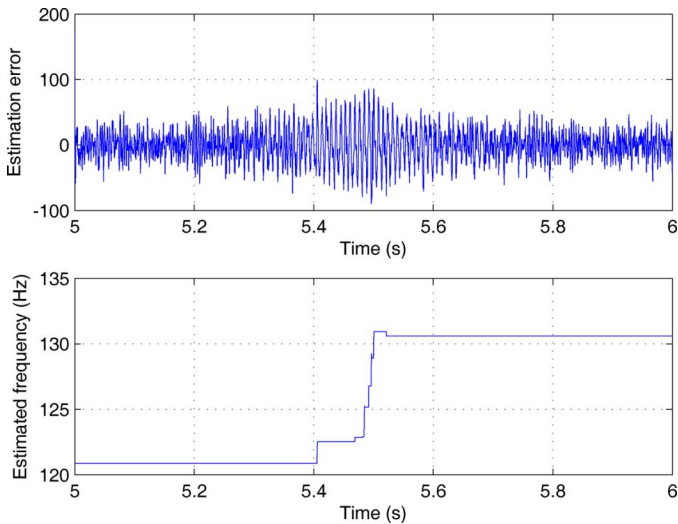


Fig. 14. Data from the adaptive scheme when the loop is closed at 5 s, the actual modal frequency is 127.26 Hz. *Top plot:* Estimation error. *Bottom plot:* Estimated modal frequency.

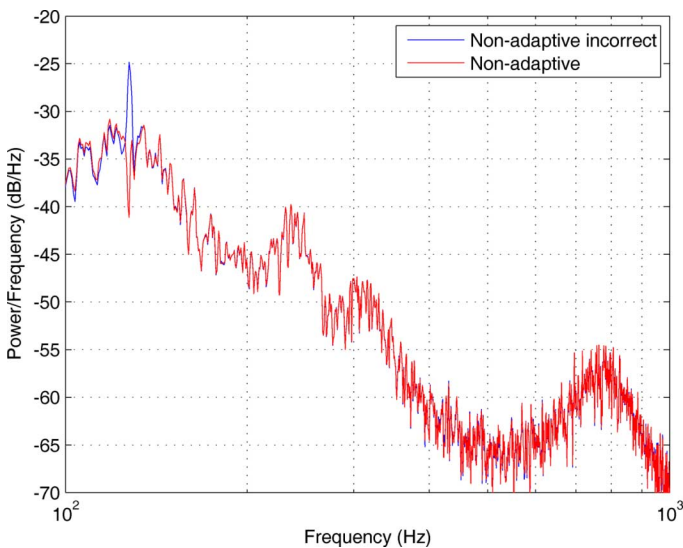


Fig. 15. PSDs computed from experimental data comparing a non-adaptive notch filter with an incorrect center frequency (97% of nominal) and one which is correct.

The adaptive mode suppression scheme does not guarantee that $\hat{\theta} = \theta^*$.

Another case of the non-adaptive scheme is run, but this time the non-adaptive notch filter's center frequency is displaced. The center frequency is set at 97% of the plant mode frequency and the system remains stable, however the standard deviation of the tracking error is increased by 10%. This is due to the lightly damped mode being excited by the control system which can be seen in Fig. 15. The plot shows the PSDs of the two cases, where the plant mode at 127 Hz can be seen as a spike in the plot due to the incorrectly placed non-adaptive notch filter.

These experimental results show that the adaptive scheme is able to provide better performance than the non-adaptive version even when the non-adaptive notch filter is centered exactly on the flexible mode. With the center frequency slightly per-

turbed the non-adaptive scheme remains stable, however there is a degradation in tracking error. The adaptive scheme can track and adjust for such an incorrect plant model, only after estimation error has sufficient information for adaptation to occur.

V. CONCLUSION

This brief presented an adaptive mode suppression scheme which incorporates an adaptive notch filter. An estimator using plant parameterization is used to track the modal frequency of the flexible dynamics of the plant. This frequency estimate is then used to update the center frequency of the adaptive notch filter. Since the adaptive notch filter will track the flexible mode, it can be designed narrower, which will allow for an increase in bandwidth of the closed loop system. The adaptive scheme is compared to a non-adaptive scheme empirically through the use of a laser beam pointing system. The experimental setup displays a plant with a lightly damped flexible mode near the desired closed loop bandwidth. Starting with incorrect parameters, the estimator of the adaptive scheme is able to track the modal frequency of the plant in real-time and results in the adaptive notch filter being able to suppress the flexible mode. The benefit of the narrow adaptive notch filter is seen in the improved tracking performance of the laser beam system. This experiment is meant to be a single example of how the adaptive mode suppression scheme may be designed and implemented as a real-time control system.

REFERENCES

- [1] J. M. T-Romano and M. Bellanger, "Fast least square adaptive notch filtering," *IEEE Trans. Acoust., Speech, Signal Process.*, vol. 36, no. 9, pp. 1536–1540, Sep. 1988.
- [2] P. A. Regalia, "An improved lattice-based adaptive IIR notch filter," *IEEE Trans. Acoust., Speech, Signal Process.*, vol. 39, no. 9, pp. 2124–2128, Sep. 1991.
- [3] M. V. Dragosevic and S. S. Stankovic, "An adaptive notch filter with improved tracking properties," *IEEE Trans. Signal Process.*, vol. 43, no. 9, pp. 2068–2078, Sep. 1995.
- [4] K. Ohno and T. Hara, "Adaptive resonant mode compensation for hard disk drives," *IEEE Trans. Ind. Eng.*, vol. 53, no. 2, pp. 624–630, Apr. 2006.
- [5] M. J. Englehart and J. M. Krauss, "An adaptive control concept for flexible launch vehicles," presented at the AIAA Guid., Nav. Control Conf., Hilton Head, SC, Aug. 1992.
- [6] R. K. Mehra and R. K. Prasad, "Time-domain system identification methods for aeromechanical and aircraft structural modeling," *J. Aircraft*, vol. 41, no. 4, pp. 721–729, Jul. 2004.
- [7] T. W. Lim, A. Bosse, and S. Fisher, "Adaptive filters for real-time system identification and control," *J. Guid., Control, Dyn.*, vol. 20, no. 1, pp. 61–66, Jan. 1997.
- [8] S.-C. Wu and M. Tomizuka, "Repeatable runout compensation for hard disk drives using adaptive feedforward cancellation," in *Proc. Amer. Control Conf.*, Minneapolis, MN, Jun. 2006, pp. 382–387.
- [9] P. Ioannou and B. Fidan, *Adaptive Control Tutorial*. Philadelphia, PA: SIAM, 2006.
- [10] N. O. Pérez-Arancibia, J. S. Gibson, and T.-C. Tsao, "Frequency-weighted minimum-variance adaptive control of laser beam jitter," *IEEE/ASME Trans. Mechatron.*, vol. 14, no. 3, pp. 337–348, Jun. 2009.
- [11] J. Levin, P. Ioannou, and M. Mirmirani, "Adaptive mode suppression scheme for an aeroelastic airbreathing hypersonic cruise vehicle," presented at the AIAA Guid., Nav. Control Conf., Honolulu, HI, Aug. 2008.
- [12] J. Levin and P. Ioannou, "Adaptive mode suppression and disturbance rejection scheme with application to disk drives," *IEEE Trans. Control Syst. Technol.*, vol. 17, no. 3, pp. 620–632, May 2009.
- [13] F. Franklin, J. Powell, and M. Workman, *Digital Control of Dynamic Systems*. Boston, MA: Addison-Wesley, 1990.